Nanoflakes like Bi doped ZnO nanostructures prepared via Co-Precipitation approach for the enhancement of dye degradation

S. JAGADHESAN[a], V. SENTHILNATHAN[b], T. S. SENTHIL[c,*]
[a]*Department of Physics, Easa College of Engineering and Technology, Coimbatore-641105, India*
[b]*Department of Physics, Government Arts College, Udumalpet – 642126, India*
[c]*Department of Physics, Erode Sengunthar Engineering College, Thudupathi, Erode-638476, India*

In the present work, pure zinc oxide (ZnO) nanoparticles (NPs) and flakes like structured Bismuth (Bi) doped ZnO nanostructures (NSs) were prepared by simple co-precipitation approach. Purity of the prepared material and the presence of various functional groups in the synthesized materials are confirmed by powder X-ray diffraction (PXRD) and Fourier Transform Infrared Spectroscopy (FTIR) analysis. The structure and morphology of Bi (0.02%, 0.04% & 0.06%) doped ZnO NSs were determined by using Field Emission Scanning Electron Microscopy (FESEM) and the presence of elemental composition in the synthesized samples were identified by Energy Dispersive X-ray spectroscopy (EDAX) analysis. The photo-catalytic activity of Bi (0.02%, 0.04% and 0.06%) doped ZnO NSs was studied for methylene blue dye degradation.

(Received November 8, 2017; accepted June 7, 2018)

Keywords: Nanoflakes, Co-precipitation, Photo-catalytic activity

1. Introduction

In recent years, increased industrialization makes a serious threat to human health in the form of environmental pollution. In recent years, ZnO nanomaterials fascinate the researchers due to its unique physical and chemical properties [1]. However, the ZnO NPs having high excitonic binding energy (~60 meV), n-type semiconductor with a wide band gap energy (3.37 eV), and this enhanced property to be used in various applications such as biosensors, gas sensors, nanogenerators and varistors [2]. And also, ZnO is a better candidate for the photo-catalytic degradation of organic pollutants present in water [3]. Generally, ZnO nanomaterial was synthesized by hydrothermal method, co-precipitation method, sol-gel method, biosynthesis method and sono-chemical method [1, 3]. Among them, Co-precipitation method is important for the production of ZnO nanoparticles in large volume. Because, the shape and size of the synthesized particles can be easily controlled by altering the pH of the medium [2].

In recent trends, doping is very useful technique to improve the charge separation in the semiconductor system [4]. Doping of ZnO material has good optical and electrical properties to be adapted, through alteration of its electronic structure and band gap [5]. Many dopant materials are used to enhance the photo-catlytic activity of ZnO nanoparticles [4]. So, in our present study we focused the importance of Bi doped ZnO NSs prepared via co-precipitation approach for the enhancement of dye degradation process and Methelyne Blue (MB) dye was used as a model pollutant.

2. Experimental

2.1. Materials for synthesis of pure and Bi doped ZnO NS

The Zinc sulfate Heptahydrate ($ZnSO_4 \cdot 7\ H_2O$), Sodium Hydrogen Carbonate ($NaHCO_3$) and Bismuth nitrate ($Bi(NO_3)_3 \cdot 5H_2O$) were used for the synthesis of Bi doped ZnO. Methylene blue (MB) dye was used for the photo-degradation process and all the chemicals were used in analytical grade and purchased from Merck.

2.2. Synthesis of pure ZnO NPs

In each 100 ml of double distilled (DD) water, 30 ml zinc sulfate heptahydrate ($ZnSO_4 \cdot 7H_2O$) and 30 ml sodium hydrogen carbonate ($NaHCO_3$ solution) was taken. After that diluted sodium hydrogen carbonate solution was added drop wise into the diluted solution of zinc sulfate heptahydrate in aqueous condition and stirred that solution at 30 min. After stirring, the solution was washed several times with DD water. Finally, the obtained white precipitate was dried in hot air oven at 150ºC for 1h and annealed at 450°C for 3h. During the drying process, $Zn(OH)_2$ fully conversion into ZnO NPs. Finally, pure ZnO NPs was taken into further characterization.

2.3. Synthesis of Bi doped ZnO NSs

Firstly, 100 ml of 0.1 M zinc sulfate heptahydrate was taken and then doping material of bismuth nitrate

$[Bi(NO_3)_3 \cdot 5H_2O]$ (0.02%, 0.04% & 0.06%) was slowly added into the zinc sulfate heptahydrate solution. Then 20 ml sodium hydrogen carbonate was added drop wise to the above mentioned solution. The colour was turned into white colour. After that the solutions were centrifuged and dried at 100°C for 6 h followed by annealing at 450°C for 3h. Finally, the obtained Bi doped ZnO NPs were used for further characterization.

2.4. Photo-catalytic dye degradation studies

The photo-catalytic activity of as synthesized pure and Bi (0.02 %, 0.04 % and 0.06 %) doped ZnO NSs have been investigated using Methylene blue (MB) organic dye under UV light irradiation at room temperature. A 15 Watts UV lamp (Philips TUV-08) was used in this experiment. 0.03 gm of Bi (0.02 %, 0.04 % and 0.06 %) doped ZnO NSs samples were taken and it was slowly dissolved in 30 ml of 100 µm aqueous solution of MB dye. The prepared solution was kept at dark condition for accomplish the adsorption desorption equilibrium between dye and photo-catalyst. Then, the sample was irradiated using UV light source and the irradiated samples were taken at a regular time interval followed by filtration. After the filtration process, the solution was used to analyze the UV-Visible absorption behaviour of the organic dyes. The maximum absorption for MB dye was identified at $\lambda = 663$ nm in the UV-Visible absorption spectra. Degradation efficiency of the synthesized material was calculated using following formula

$$\text{Degradation efficiency} = [C_0\text{-}C_t/C_0] \text{ X } 100 = [A_0\text{-}A_t/A_0] \text{ X } 100 \quad (1)$$

where, C_0 and C_t denotes the initial concentration and concentration of dye solution at particular time interval, A_0 and A_t denotes the initial absorbance and absorbance of dye solution at regular time interval.

2.5. Characterization techniques

Morphology and sizes of the prepared nanomaterials were determined by field emission scanning electron microscope (SIGMA HV – Carl Zeiss with Bruker Quantax 200 – Z10 EDS Detector). The X-ray diffraction (XRD) patterns were recorded using a mini desktop diffractometer (X'PERT PRO MPD X-ray diffractometer) operated at an accelerating potential of 40 kV and 30 mA filament current with CuKα radiation of wavelength 1.5406 Å in a scanning rate of 3 per minute (from 2h = 10 ºC to 80 ºC). Optical absorption spectra were recorded using a UV – VIS double beam spectrometer (SYSTRONICS: AU-2707) in the range of 190–900 nm.

3. Results and discussion

3.1. X-ray diffraction analysis

The phase, purity and crystal structure of the synthesized materials were analysed from the XRD analysis. The XRD studies have wide variety of applications towards analysing crystalline structure, chemical composition, orientation and phase identification. Fig. 1 reveals the XRD pattern of different concentration of Bi (0 %, 0.02 %, 0.04 % and 0.06 %) doped ZnO NSs. The XRD spectra shows that all the diffraction peaks are well matched with hexagonal wurtzite structure of ZnO and the corresponding planes (100), (002), (101), (102), (110), (103), (200), (112) and (201) were well matched with standard JCPDS NO: 36-145 [6]. The high intensity peak such as (101) of pure ZnO decreases with increase of Bi contents and is shown in Fig 2. This decrement may happen due to the defects or incorporation of Bi ions created into the ZnO lattice structure [5, 7]. The high intense peak also shifted towards right side and it may due to the ionic radius, the ionic radius of Bi^{3+} is larger than that of Zn^{2+} ionic radius. This means doped Bi^{3+} atoms are substitute for Zn^{2+} atoms [5].

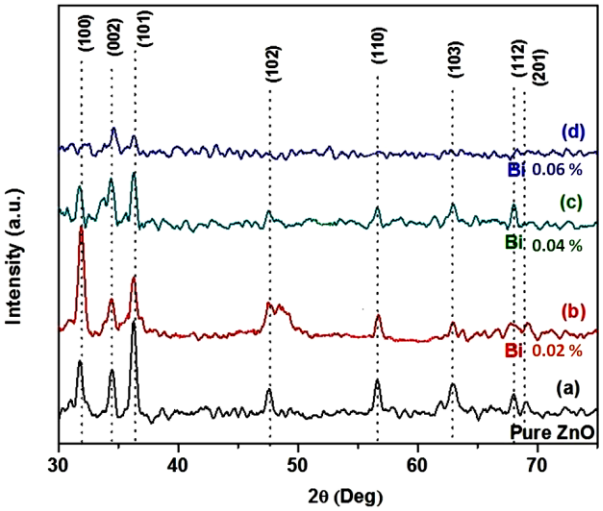

Fig. 1. XRD results of (a) Pure ZnO and (b, c & d) different concentration of Bi (0.02%, 0.04% and 0.06%) doped ZnO NSs

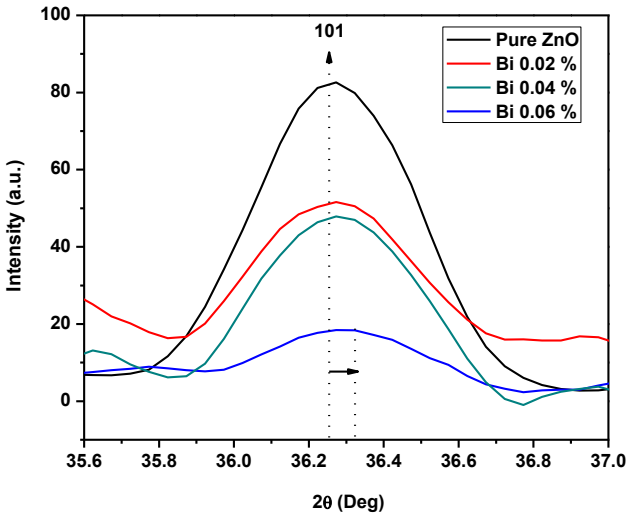

Fig. 2. Bi concentration dependent shift in (101) diffraction peak

The average crystallite size of the synthesized materials was calculated by using Scherrer's formula,

$$D=K\lambda/\beta \cos\theta \quad (2)$$

where, λ is wavelength of the X-ray beam, θ is diffraction angle, D - crystallite size, K is shape factor and β is Full Width Half Maximum (FWHM) of the peak. The average crystallite size values are found to 55, 59, 64 and 68 nm for pure ZnO and Bi (0.02 %, 0.04 % and 0.06 %) doped ZnO NSs respectively.

3.2. Fourier transform infrared spectroscopy (FT-IR)

The FTIR spectra shows the effect of complexing agents on precursors used to synthesize Bi (0%, 0.02 %, 0.04 % and 0.06 %) doped ZnO NSs and the spectra was recorded by using Perkin-Elmer spectrometer in the range between 4000-400 cm^{-1} using KBr pellet techniques. The bands around at 400–600 cm^{-1} indicates the formation of ZnO nanostructure. Fig. 3 reveals the FTIR spectrum of pure ZnO and Bi (0.06 %) doped ZnO NSs. A small peak at 2934 cm^{-1} indicates CH_2 asymmetric stretching vibration [5]. The peak observed at 2360 cm^{-1} indicates the presence of CO_2 molecule present in air medium [2]. The band at 1633 cm^{-1} ascribed H–O–H bending vibrations possibly including water (H_2O) content [5].The band at 1121 cm^{-1} is the sulphate group comes from the precursor material [2]. A small peak observed at 474 cm^{-1} indicates the bending vibration of Zn-O stretching and the peak at 670 cm^{-1} is attributed to Bi–O stretching [2, 5]. So, this Bi-O stretching may occur owing to Bi ions replaced by Zn ions in ZnO crystal lattice [2, 5].

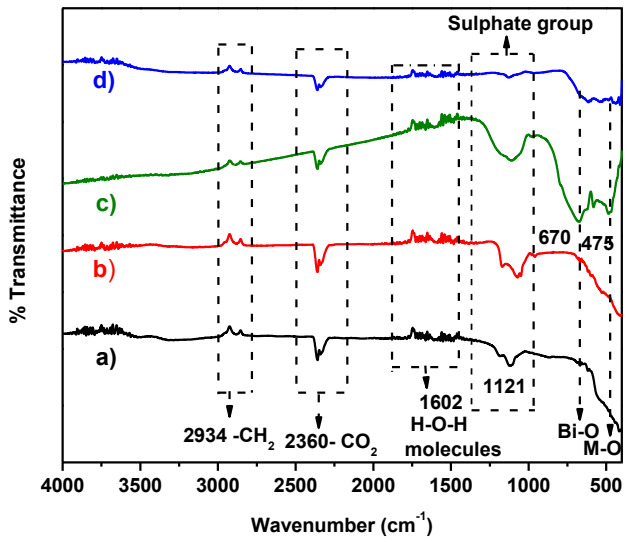

Fig. 3. FTIR spectrum of (a) Pure ZnO and (b) Bi (0.02%, 0.04% & 0.06%) doped ZnO NSs

3.3. UV-visible spectroscopy

The UV-Visible absorbance spectra analysis was used to study about the optical property of synthesized sample. Fig. 4 shows the UV-Visible absorption spectra of Bi (0%, 0.02 %, 0.04 % & 0.06 %) doped ZnO NSs. The absorbance wavelength of Bi (0%, 0.02 %, 0.04 % & 0.06 %) doped ZnO was observed at 300 nm, 305 nm, 303 nm, and 307 nm respectively. The band gap of the prepared material was estimated by using Tauc's relation

$$(\alpha h\upsilon)^n=A*(h\upsilon-E_g) \quad (3)$$

where, hυ is the UV light energy, E_g is the optical band gap of the semiconductor and n represents the optical transition [9]. The optical transition (n) have specific values such as 1/2, 2, 3/2 or 3 respectively for the direct, indirect, forbidden direct or forbidden indirect transitions. The direct band gap of Bi (0%, 0.02 %, 0.04 % and 0.06 %) doped with ZnO samples were determined by $(\alpha h\upsilon)^{1/2}$ vs (hυ) relation as inset Fig. 4. Where, α - is the absorbance coefficient, h- represents planks constant, υ- is the velocity of light and λ is the wave length. The direct band gap energy was found to be 3.86 eV, 3.84 eV, 3.80 eV and 3.77 eV respectively for pure ZnO and Bi (0.02 %, 0.04 % and 0.06 %) doped ZnO NSs. From the obtained results, it should be noted that band gap decrease with increase of dopant concentration. It may happen due to the various factors (i.e) oxygen stoichiometry, size effect, quantum confinement effect and enhancement of surface area to volume ratio [10].

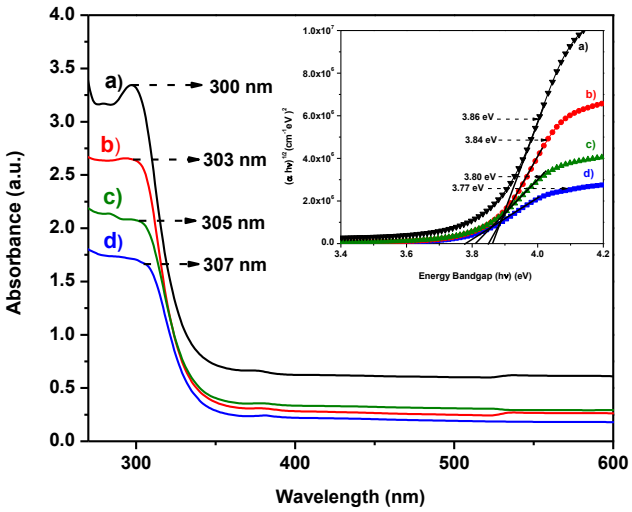

Fig. 4. UV-Vis spectrum and Tauc's plot of (a) pure ZnO and (b, c & d) Bi (0.02%, 0.04% & 0.06%) doped ZnO NSs

3.4. Morphological studies

Fig. 5 (a, b, c & d) shows the different magnification of FESEM analysis of pure ZnO and flake like structured Bi (0.02 %, 0.04 % and 0.06 %) doped ZnO NSs. The

image was recorded by using the instrument of JEOL JS-6390 combined with an EDAX spectrometer.

Fig. 5(a) clearly shows that the ZnO NPs were agglomerated and look like a spherical in shape. But, Bi (0.02 %, 0.04 % and 0.06 %) doped ZnO NSs are looks flake like structure. The Bi (0.06%) doped ZnO sample shows clearly that the nanoflakes are formed uniformly compared with Bi (0.02% & 0.04%) doped ZnO.

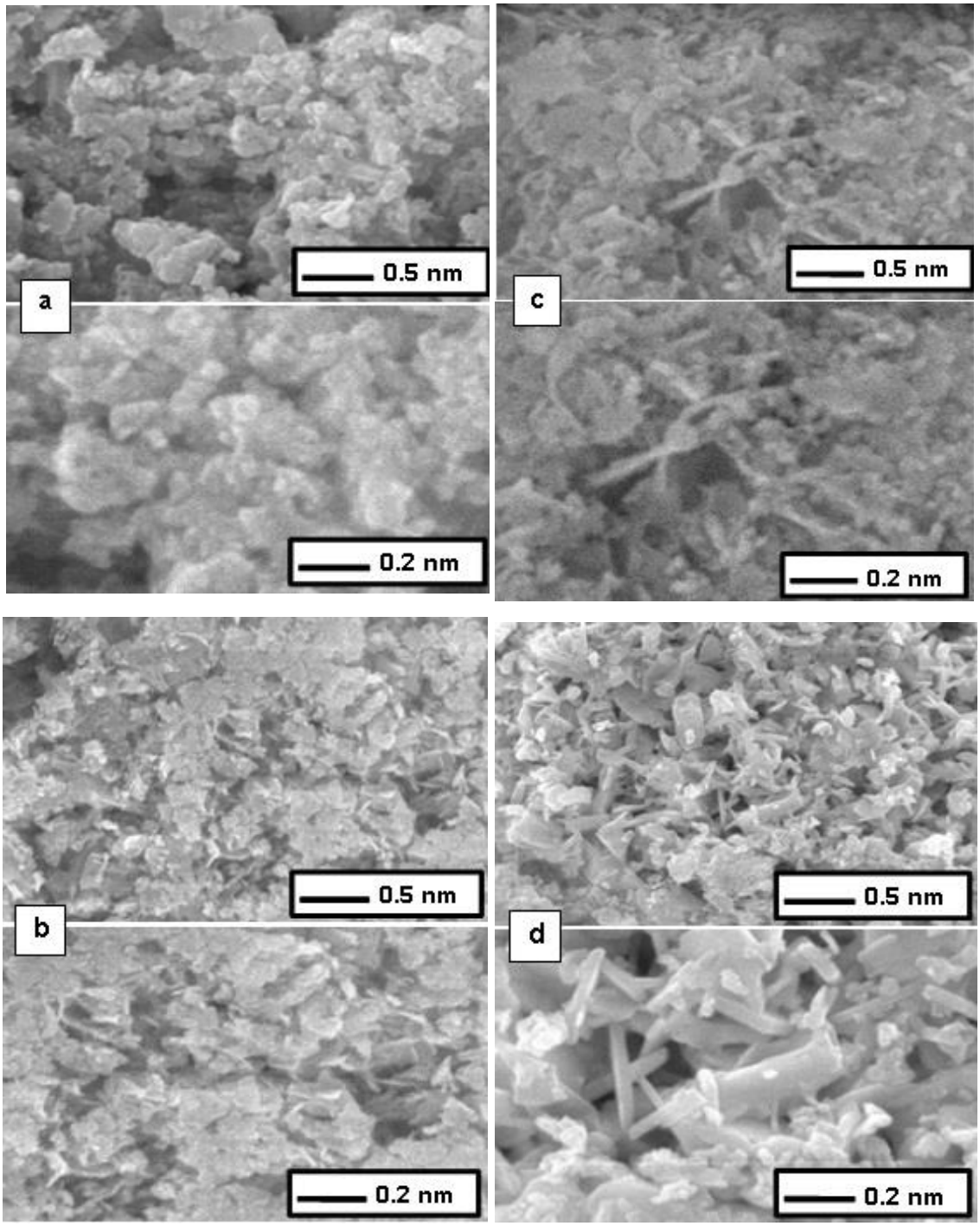

Fig. 5. Surface morphology of (a) Pure ZnO, (b, c & d) different concentration of flake like Bi (0.02%, 0.04% and 0.06%) doped ZnO NSs

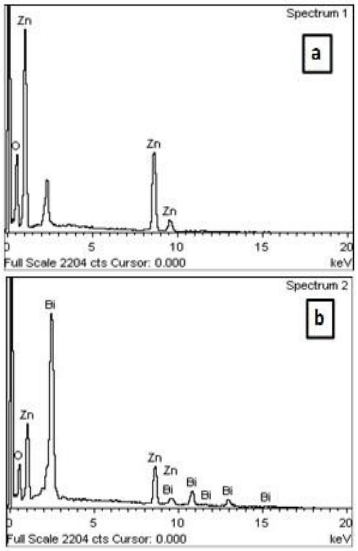

Fig. 6. EDAX spectrum for (a) pure ZnO and (b) Bi doped ZnO NSs

Fig. 6 (a & b) shows the EDAX spectrum of pure ZnO NPs and Bi (0.06 %) doped ZnO NSs. The pattern shows that the prepared samples has a composition of Zn-48.74 at %, O-51.26 at %, which confirmed that Zn, O elements presents in the pure ZnO sample without any impurities. Whereas, Fig. 6 (b) clearly shows the presence of Bi on the prepared samples with the composition of Bi-1.06 at %.

3.5. MB dye degradation studies

The photo-catalytic activity of Bi (0.02%, 0.04% and 0.06%) doped ZnO NSs was evaluated through MB dye under UV light. Fig. 7 (a, b & c) shows the time dependent UV-Vis absorption spectra for MB dye removal of 0.02%, 0.04% and 0.06 % Bi doped ZnO NSs.

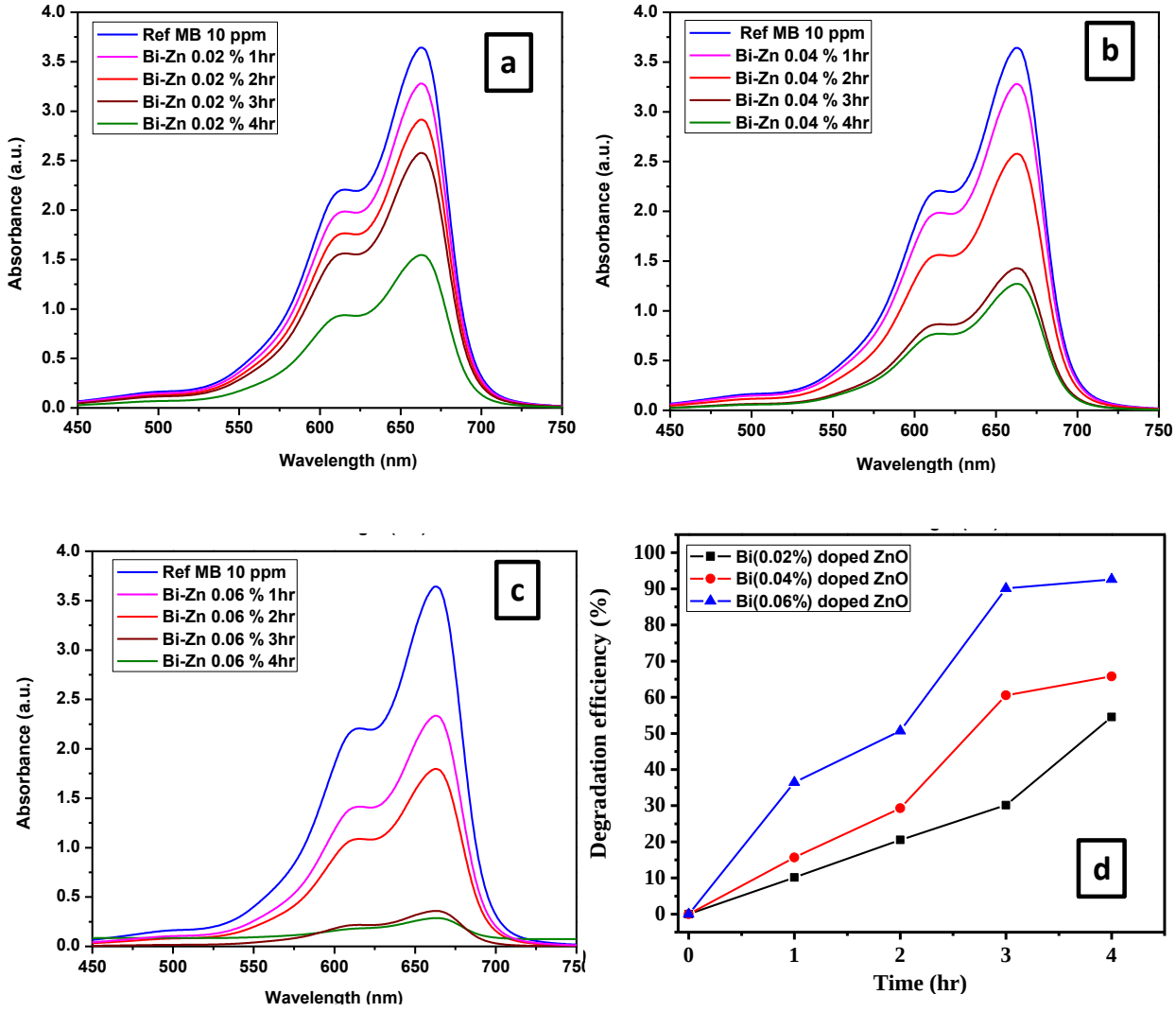

Fig. 7. (a, b & c) The time dependent UV-Vis absorption spectra for MB dye removal of 0.02%, 0.04% and 0.06 mol% Bi doped ZnO NSs (d) Dye degradation Efficiency graph for Bi (0.02%, 0.04% & 0.06%) doped ZnO NSs

From the figure, the absorption peak of MB (663 nm) decreases linearly with an increase of concentrations of (0.02%, 0.04% & 0.06%) Bi dopant. This decrease may happen owing to their Bi decoration on the surface of ZnO [11]. Fig. 7 (d) reveals that the degradation efficiency graph of Bi (0.02%, 0.04% & 0.06%) doped ZnO NSs. This higher degradation efficiency may attributed to the increase of total surface area or the presence of surface oxygen vacancies [11]. The formation of flake like structure also enhance the dye degradation with enhanced dye adsorbing area. In addition, Bi doping can suppress the recombination of electron-hole pairs due to increase their efficiency [12, 13]. From these results, we can say that the surface of Bi doped ZnO NSs material has played a vital role in dye degradation process.

4. Conclusion

Various concentrations of (0.02%, 0.04% & 0.06%) Bi doped ZnO NSs were synthesized via Co-precipitation method. The phase, purity of pure ZnO NPs and Bi (0.02%, 0.04% and 0.06%) doped ZnO NSs were confirmed by the XRD analysis. The formation of flake like structure was confirmed by SEM analysis. 0.06% Bi doped ZnO NSs shows enhanced dye degradation efficiency compare with 0.02% & 0.04% Bi doped ZnO NSs. This enhancement create owing to their large surface area and surface oxygen vacancies presence in the Bi (0.06%) doped ZnO NSs.

Acknowledgement

The author would like to thank the Science and Engineering Research Board (SERB) Sanction Order No and date: SB/FTP/PS-114/2012 Dated 17.09.2013, Department of Science and Technology, New Delhi 110 016 for the financial support.

References

[1] N. Senthilkumar, E. Nandhakumar, P. Priya, D. Soni, M. Vimalan, I. Vetha Potheher, New J. Chem. **41**, 10347 (2017).
[2] R. Jeyachitra, V. Senthilnathan, T. S. Senthil, J. Mater. Sci.: Mater. Electron. **29**(2), 1189 (2018).
[3] Rajeswari Rathnasamy, Pitchai Thangasamy, Rangasamy Thangamuthu, Sridhar Sampath, Viswanathan Alagan, J. Mater. Sci.: Mater. Electron. **28**(14), 10374 (2017).
[4] V. L. Chandraboss, L. Natanapatham, B. Karthikeyan, J. Kamalakkannan, S. Prabha, S. Senthilvelan, Materials Research Bulletin **48**(10), 3707 (2013).
[5] T. Prakash, G. Neri, A. Bonavita, E. Ranjith Kumar, K. Gnanamoorthi, J. Mater. Sci.: Mater. Electron. **26**(7), 4913 (2015).
[6] N. Senthil Kumar, M. Ganapathy, S. Sharmila, M. Shankar, M. Vimalan, I. Vetha Potheher, J. Alloys and Compounds **703**, 624 (2017).
[7] B. Joseph, P. K. Manoj, Y. K. Vaidyan, Ceramics International **32**(5), 487 (2006).
[8] M. Ohyama, H. Kozuka, T. Yoko, Am. Ceram. Soc. **81**, 1622 (1998).
[9] V. Vijayabala, N. Senthilkumar, K. Nehru, R. Karvembu, J. Mater. Sci: Mater. Electron. **29**(1), 323 (2018).
[10] M. H. Chou, S. B. Liu, C. Y. Huang, S. Y. Wu, C. L. Cheng, Applied Surface Science **254**, 7539 (2008).
[11] K. Kumar, M. Chitkara, I. S. Sandhu, D. Mehta, S. Kumar, Journal of Alloys and Compounds **588**, 681 (2014).
[12] X. Yu, D. Meng, C. Liu. K. Xu, J. Chen, C. Lu, Y. Wang, J. Mater. Sci: Mater. Electron. **25** (9), 3920 (2014).
[13] Wiem Bousslama, Habib Elhouichet, Mokhtar Ferid, Optik - International Journal for Light and Electron Optics **134**, 88(2017).

*Corresponding author: tssenthi@gmail.com